Coherent Polarization-Diversity Radar Techniques in Meteorology

J. I. METCALF AND J. D. ECHARD

Engineering Experiment Station, Georgia Institute of Technology, Atlanta 30332

(Manuscript received 27 February 1978, in final form 12 June 1978)

ABSTRACT

A coherent polarization-diversity (dual channel) radar can be used to obtain spectral functions analogous to the four parameters derived from a noncoherent polarization-diversity radar. Formulations for the two power spectra and the cross spectrum are developed theoretically, and their interpretation is illustrated by model calculations. Analytical results include the derivation of raindrop size distributions, separation of Doppler velocity components due to air velocity and raindrop fallspeed, and improved identification of hail in rain. Effects of turbulence are illustrated and propagation effects are discussed briefly. The coherent polarization-diversity radar has potential value for a wide variety of research areas, including weather modification, severe storms, precipitation microphysics and electromagnetic propagation.

1. Introduction

The coherent polarization-diversity (dual channel) radar represents a significant advance in remote measurement of meteorological parameters and has great potential benefit for a variety of research and operational problems. We have begun to develop the theory for extracting information from such a radar on the basis of spectral analysis techniques, whereby the received signals are displayed in the frequency domain, corresponding to the radial (Doppler) velocities of the scattering particles. Under appropriate conditions it is possible to obtain partial measurement of the size distribution of raindrops and to separate unambiguously the Doppler velocity components due to fallspeed and to air velocity. Identification of hail in rain is improved over the capability of a noncoherent polarization-diversity radar. These capabilities are limited in some cases by propagation effects or by turbulence. Some of these limitations are illustrated by model calculations.

The radar is assumed to be capable of transmitting a circularly polarized signal and coherently receiving signal components with circular polarizations opposite (main channel) and identical (orthogonal channel) to that of the transmitted signal. The nomenclature of the channels follows that of Barge (1972) and Humphries (1974) and is based on the fact that the backscatter from hydrometeors tends to be elliptically polarized with a sense of rotation opposite to that of the transmitted signal. Thus, the received power in the "orthogonal" channel is typically 10–40 dB lower than that in the "main" channel. This nomenclature differs from that generally used in nonmeteorological radar applications where the transmitter channel is designated the "main" receiver channel.

0022-4928/78/2010-2019$05.00

2. Background

In the past decade considerable research has been directed toward the interpretation of meteorological data from coherent single-channel radars and from noncoherent polarization-diversity radars. In particular, power spectra from coherent (Doppler) radars have been used to infer hydrometeor size distributions (duToit, 1967; Sekhon and Srivastava, 1971; Battan and Theiss, 1972) and to obtain information on microscale processes such as those at the base of cloud layers (Harris, 1977). Interpretation of Doppler spectra in terms of drop size distributions involves approximations which often limit the validity of the results. Another application of coherent radars is the use of Doppler velocity data for storm dynamics research (e.g., Kropfli and Miller, 1976). Attempts have been made to incorporate Doppler radar data into storm models and to compute three-dimensional wind fields from simultaneous dual-radar measurements. In such applications the value of data obtained at high radar elevation angles is limited by the difficulty of separating the Doppler velocity components due to fallspeed and air velocity.

Operational requirements for the detection of hail in thunderstorms and the measurement of electromagnetic propagation parameters in precipitation have led to research programs involving noncoherent polarization-diversity (dual channel) radars for these purposes. The four parameters that can be derived from a circularly polarized polarization-diversity radar were first described by McCormick (1968) and, subsequently, by Barge (1972), Humphries (1974) and McCormick and Hendry (1975). These include the average power in each of the receiver channels (or the main channel power and the circular depolarization ratio) and the magnitude

and phase of the cross correlation at zero time lag between the two channels. The derivation and interpretation of these quantities have been discussed extensively in the meteorological and electrical engineering literature. It should be noted that the "phase" measurement reported by these authors is the *relative* phase between the two receiver channels, which does not require a coherent phase reference in the receiver.

A limited amount of research has been devoted to the measurement and interpretation of data from coherent polarization-diversity radars. Chernikov *et al.* (1973) reported "remarkable" differences in observed Doppler spectra from orthogonal polarizations measured with a 3.2 cm radar but to our knowledge they have not published these data. Battan and Theiss (1975) reported observations of Doppler spectra measured sequentially in the main and orthogonal channels of their linearly polarized vertically pointing 3.2 cm radar. More data of this type were presented by Battan (1977) and used in an analysis of hydrometeor microphysics.

The interpretation of Doppler spectra obtained simultaneously from a polarization-diversity radar was discussed theoretically by Warner and Rogers (1977). They developed a model of rain to simulate Doppler spectra of signals in the main and orthogonal channels of a circularly polarized radar receiver and to show the dependence of the spectra on rainfall rate, fraction of preferentially oriented drops, Doppler variance and radar elevation angle. These results deal only with the power spectra and not the cross spectrum of the two received signals. The techniques we present are based on combined use of the two power spectra and the cross spectrum.

Because our formulations of the spectral functions are based substantially on the theory for noncoherent polarization-diversity radars, it is essential to summarize those results. We follow the notation of Humphries (1974). The received signals E_1 and E_2 in the orthogonal and main channels, which are identical and opposite, respectively, to the sense of the circularly polarized transmission, are given by

$$E_1=\exp(j2\pi f_0 t)\sum_{i=1}^{N} E_{1i}$$

$$=\exp(j2\pi f_0 t)\sum_{i=1}^{N}[\exp(-2jkr_i)/2r_i^2](S_{11i}+S_{22i})$$

$$\times\{\nu_i\exp[j(\delta_i\pm 2\alpha_i)]+2p\exp[j(\chi\pm 2\tau)]\}, \quad (1)$$

$$E_2=\exp(j2\pi f_0 t)\sum_{i=1}^{N} E_{2i}$$

$$=\exp(j2\pi f_0 t)\sum_{i=1}^{N}[\exp(-2jkr_i)/2r_i^2](S_{11i}+S_{22i}), \quad (2)$$

where E_{1i} and E_{2i} are the received components in the orthogonal and main channels due to the ith scatterer, f_0 is the carrier frequency, r_i is the range to the ith scatterer, S_{11i} and S_{22i} are the diagonal elements in the scattering matrix relative to the symmetry axis of the scatterer (so that S_{12i} and S_{21i} are zero for a symmetrical scatterer or are incorporated into the parameter δ_i for an unsymmetrical scatterer), α_i is the inclination to the vertical of the symmetry axis of the scatterer (the canting angle), δ_i is the differential phase shift on scattering (due to non-Rayleigh scattering) between the major and minor axes of the scatterer, and ν_i is the ratio of backscattered amplitudes in the orthogonal and main channels from the ith scatterer. The propagation term is based on a model of an anisotropic (precipitation-filled) medium with symmetry axes rotated through an angle τ from the vertical and horizontal. The other propagation parameters are defined by

$$k=(k'+k'')/2, \quad (3)$$

$$pe^{j\chi}=\tanh[j(k''-k')r/2], \quad (4)$$

where k' and k'' are the propagation constants along the symmetry axes of the propagation medium. The latter quantity can alternately be expressed in terms of the total one-way differential attenuation ΔA and differential phase shift $\Delta\phi$ in the medium:

$$pe^{j\chi}=\tanh[0.0575\Delta A+j(\pi/360)\Delta\phi]. \quad (5)$$

The upper and lower signs in Eq. (1) correspond to the transmission of right and left circular polarization, respectively.

The origin of the two components of backscatter can be visualized by resolving the circularly polarized transmitted signal into linear components of equal amplitude in planes parallel and perpendicular to the symmetry axis of the scatterer. The component parallel to the axis is reflected with an amplitude S_{11i} and the component perpendicular to the axis is reflected with an amplitude S_{22i}. The backscattered signal is thus elliptically polarized with axes proportional to S_{11i} and S_{22i} and orientation corresponding to the orientation of the scatterer. If the ellipse is resolved into two components having opposite circular polarizations, the component with polarization opposite to that of the transmitted signal has an amplitude proportional to $S_{11i}+S_{22i}$ and the component with polarization identical to that of the transmitted signal has an amplitude proportional to $S_{11i}-S_{22i}$. The amplitude ratio ν_i is introduced in order to express both circular components in terms of the sum of the scattering amplitudes. If the scatterer is spherical, then $S_{11i}=S_{22i}$ and no signal is received in the transmission channel.

Four parameters derived from these signals in a noncoherent radar are the two average intensities

$$W_1=\langle E_1E_1^*\rangle, \quad (6)$$

$$W_2=\langle E_2E_2^*\rangle, \quad (7)$$

and the magnitude and phase of the cross-correlation

function at zero time lag, which is given by

$$\frac{W}{(W_1W_2)^{\frac{1}{2}}}=\frac{\langle E_1E_2^*\rangle}{(\langle E_1E_1^*\rangle\langle E_2E_2^*\rangle)^{\frac{1}{2}}}=|\rho|e^{j\Phi}. \tag{8}$$

McCormick (1968) suggested a model of the hydrometeor array having a fraction ρ_α with a fixed orientation angle $\bar{\alpha}$ and mean scattering parameters $\bar{\nu}$ and $\bar{\delta}$, plus a fraction $1-\rho_\alpha$ which are randomly oriented with a uniform distribution. The oriented fraction contributes to the cross correlation, whereas the contributions due to the randomly oriented scatterers are mutually cancelling. Humphries (1974) showed that the magnitude of the cross correlation is given by

$$|\rho|=\frac{|\rho_\alpha\bar{\nu}\exp[j(\bar{\delta}\pm2\bar{\alpha})]+2p\exp[j(\chi\pm2\tau)]|}{\{|\overline{\nu\exp[j(\delta\pm2\alpha)]+2p\exp[j(\chi\pm2\tau)]}|^2\}^{\frac{1}{2}}}, \tag{9}$$

where the averaging denoted by the overbar is over the scattering array. In an isotropic medium, where $p=0$, Eq. (9) reduces to

$$|\rho|=\frac{\rho_\alpha|\bar{\nu}\exp[j(\bar{\delta}\pm2\bar{\alpha})]|}{\{|\overline{\nu\exp[j(\delta\pm2\alpha)]}|^2\}^{\frac{1}{2}}}=\rho_\alpha\frac{\bar{\nu}}{[\overline{\nu^2}]^{\frac{1}{2}}}. \tag{10}$$

Thus the magnitude of the cross correlation is a measure of the fraction of oriented scatterers, and in general $|\rho|\leqslant\rho_\alpha$. In an isotropic medium, the phase of the cross correlation is related to the orientation by

$$\Phi=\bar{\delta}\pm2\bar{\alpha}. \tag{11}$$

The cross correlation at zero time lag is a valuable parameter for deducing properties of the scattering medium. Radar measurements at 1.8 and 10 cm (Anderson, 1975; Hendry *et al.*, 1976) have shown that rain is a strongly oriented medium ($|\rho|=0.6$ to 0.9), whereas hail and snow appear to be randomly oriented ($|\rho|<0.4$). The phase of the cross correlation is useful in the identification of large hydrometeors, e.g., hail, if the differential phase shift $\bar{\delta}$ can be determined from measurements with alternating right and left circularly polarized transmission. The circular depolarization ratio, defined as W_1/W_2, is a measure of the reflectivity-weighted ellipticity of the scatterers and, in conjunction with the reflectivity derived from W_2, is useful in determining the average size or shape and hence the thermodynamic phase of the hydrometeors. These characteristics of the derived parameters are analogous to characteristics of the spectral functions which can be derived from a coherent polarization-diversity radar.

3. Spectral formulations

The development of formulas for the spectral functions is based on Eqs. (1) and (2) above. We form the autocovariance function of each of the received signals and the cross-covariance function of the two signals. The spectra and the cross spectrum are the Fourier transforms of the autocovariance functions and the cross-covariance function, respectively.

Potential confusion exists in the nomenclature of the cross spectrum, due to the fact that the receiver channel orthogonal to the transmission channel is sometimes referred to as the "cross-polarized channel" or "cross channel." We emphasize the definitions of the receiver channels given in the Introduction and the definitions of the spectral functions given above.

The most general formulation of the spectral functions involves the time-dependence of all of the parameters in Eqs. (1) and (2) which carry the subscript i. The propagation parameters p, χ and τ can be assumed to vary much more slowly than the scattering parameters, since they are integrated over the propagation path. The physical significance of the time-dependence of the parameters is as follows. The range $r_i(t)$ varies according to the radial movement of the scatterer. The scattering matrix amplitudes $S_{11i}(t)$ and $S_{22i}(t)$ and the ratio $\nu_i(t)$ vary as a result of inertial oscillations of raindrops, as investigated by Musgrove and Brook (1975). The variations in the sum of the scattering amplitudes are much less than those in the ratio ν_i, so that the effects of these oscillations should appear only in the orthogonal channel signal E_1. The orientation angle $\alpha_i(t)$ changes due to tumbling of the scatterers. It can also change due to inertial oscillations, since it would alternate between a value near zero for an oblate shape and a value near 90° for a prolate shape. Time variations of $\delta_i(t)$ are difficult to formulate, but could result from tumbling of large irregular scatterers.

If the signals are assumed to be jointly stationary, the autocovariance functions are given by

$$\begin{aligned}R_{11}(t')&=\langle E_1(t)E_1^*(t+t')\rangle\\&=\langle\exp(j2\pi f_0t)\sum_i\{\exp[-2jkr_i(t)]/2r_i^2(t)\}(S_{11i}+S_{22i})\{\nu_i(t)\exp\{j[\delta_i(t)\pm2\alpha_i(t)]\}+2p\exp[j(\chi\pm2\tau)]\}\\&\times\exp[-j2\pi f_0(t+t')]\sum_l\{\exp[2jk^*r_l(t+t')]/2r_l^2(t+t')\}(S_{11l}+S_{22l})^*\{\nu_l(t+t')\exp\{j[\delta_l(t+t')\pm2\alpha_l(t+t')]\}\\&\qquad+2p\exp[j(\chi\pm2\tau)]\}^*\rangle,\end{aligned} \tag{12}$$

$$\begin{aligned}R_{22}(t')&=\langle E_2(t)E_2^*(t+t')\rangle\\&=\langle\exp(j2\pi f_0t)\sum_i\{\exp[-2jkr_i(t)]/2r_i^2(t)\}(S_{11i}+S_{22i})\\&\times\exp[-j2\pi f_0(t+t')]\sum_l\{\exp[2jk^*r_l(t+t')/2r_l^2(t+t')\}\times(S_{11l}+S_{22l})^*\rangle.\end{aligned} \tag{13}$$

The cross-covariance function is given by

$$R_{12}(t') = \langle E_1(t) E_2^*(t+t') \rangle$$
$$= \langle \exp(j2\pi f_0 t) \sum_i \{\exp[-j2kr_i(t)]/2r_i^2(t)\} (S_{11i}+S_{22i})[\nu_i(t) \exp\{j[\delta_i(t) \pm 2\alpha_i(t)]\} + 2p \exp[j(\chi \pm 2\tau)]]$$
$$\times \exp[-j2\pi f_0(t+t') \sum_l \{\exp[2jk^* r_l(t+t')]/2r_l^2(t+t')\} (S_{11l}+S_{22l})^* \rangle. \quad (14)$$

In order to simplify the ensuing mathematics we assume that inertial oscillations and tumbling can be neglected. This implies that $\nu_i(t+t') = \nu_i(t)$, $\delta_i(t+t') = \delta_i(t)$ and $\alpha_i(t+t') = \alpha_i(t)$. We acknowledge that the neglect of oscillations is not strictly valid for raindrops and that the neglect of tumbling is not generally valid for ice-phase hydrometeors, but these assumptions are used for mathematical convenience. The neglect of oscillation implies that drops of a given size return signals characteristic of an average shape related to that size. The neglect of tumbling requires that each individual scatterer not change orientation; different fixed orientations of different scatters are allowed, thus enabling us to characterize the scattering medium as having some fraction of preferentially oriented scatterers. The time-dependence of range can be expressed as $r_i(t+t') = r_i(t) - v_i t'$, where v_i is the radial velocity of the ith scatter, defined as positive toward the radar.

Following the notation of Humphries (1974) we define

$$B_i \equiv \exp[-2jkr_i(t)]/2r_i^2(t). \quad (15)$$

Because the increment of range $v_i t'$ is much less than the range $r_i(t)$, we make the approximation $r_i^2(t) \approx r_i^2(t+t')$ in the denominator of Eqs. (12), (13) and (14). With this approximation and the assumption that the scatterers are randomly distributed in range, the products $B_i B_l$ average to zero for $i \neq l$. Expressing the propagation constant in terms of its real and imaginary parts $k = k_R - jk_I$, we have

$$|B_i|^2 = \exp[-4k_I r_i(t)]/4r_i^4(t). \quad (16)$$

Noting that $\exp(2k_I v_i t') \approx 1$, we have the approximation $\exp(-2jk^* v_i t') \approx \exp(-2jk_R v_i t')$. With the above substitutions and approximations Eqs. (12), (13) and (14) become

$$R_{11}(t') = \langle \exp(-j2\pi f_0 t') \sum_i |B_i|^2 |S_{11i}+S_{22i}|^2 \exp(-2jk_R v_i t') |\nu_i \exp[j(\delta_i \pm 2\alpha_i)] + 2p \exp[j(\chi \pm 2\tau)]|^2 \rangle, \quad (17)$$

$$R_{22}(t') = \langle \exp(-j2\pi f_0 t') \sum_i |B_i|^2 |S_{11i}+S_{22i}|^2 \exp(-2jk_R v_i t') \rangle, \quad (18)$$

$$R_{12}(t') = \langle \exp(-j2\pi f_0 t') \sum_i |B_i|^2 |S_{11i}+S_{22i}|^2 \exp(-2jk_R v_i t') [\nu_i \exp[j(\delta_i \pm 2\alpha_i)] + 2p \exp[j(\chi \pm 2\tau)]] \rangle. \quad (19)$$

The only random process in Eqs. (17), (18) and (19) is the range to the ith scatterer $r_i(t)$ which occurs in the term $|B_i|^2$. Because the range cell being observed is small as compared to the range to the cell r_0, the expected value of $|B_i|^2$ can be approximated as

$$\langle |B_i|^2 \rangle \approx |B_0|^2, \quad (20)$$

where from Eq. (16),

$$|B_0|^2 = \exp(-4k_I r_0)/4r_0^4. \quad (21)$$

The spectral functions are related to the covariance functions by the Fourier transform

$$S(f) = \int_{-\infty}^{\infty} \exp(-2j\pi f t') R_{xx}(t') dt'. \quad (22)$$

From the autocovariance functions we obtain the power spectral densities or spectra of the signals in the orthogonal and main channels, i.e.,

$$S_1(f) = |B_0|^2 \sum_i |S_{11i}+S_{22i}|^2 |\nu_i \exp[j(\delta_i \pm 2\alpha_i)] + 2p \exp[j(\chi \pm 2\tau)]|^2 \delta(2\pi f_0 + 2k_R v_i + 2\pi f), \quad (23)$$

$$S_2(f) = |B_0|^2 \sum_i |S_{11i}+S_{22i}|^2 \delta(2\pi f_0 + 2k_R v_i + 2\pi f). \quad (24)$$

From the cross-covariance function we obtain the cross-spectrum

$$S_{12}(f) = |B_0|^2 \sum_i |S_{11i}+S_{22i}|^2 \{\nu_i \exp[j(\delta_i \pm 2\alpha_i)] + 2p \exp[j(\chi \pm 2\tau)]\} \delta(2\pi f_0 + 2k_R v_i + 2\pi f). \quad (25)$$

In Eqs. (23), (24) and (25) the quantity $\delta(2\pi f_0+2k_R v_i+2\pi f)$ is the Dirac delta function. According to Eqs. (23), (24) and (25) the spectral component due to the ith scatterer, moving toward the radar with a velocity v_i, appears at a frequency $f=-(f_0+k_R v_i/\pi)=-(f_0+2v_i/\lambda_0)$, where $\lambda_0=2\pi/k_R$ is the carrier wavelength. The received frequency is thus increased in magnitude by the Doppler frequency $f_d=2v_i/\lambda_0$. The negative sign for the frequency is the result of the arbitrary sign convention in the phase term $\exp[j(2\pi f_0 t-2kr_i)]$ in Eqs. (1) and (2) and in subsequent expressions based on these. The spectra and cross spectrum can be expressed as functions of Doppler velocity by the change of variables $S_v(v)dv=S(f)df$.

4. Interpretation of the spectral functions

In order to illustrate the extraction of information from the spectral functions, we assume that the propagation medium is isotropic ($p=0$) and express the spectra and cross spectrum in terms of functions of particle size. In the case of rain, the scattering cross section $\sigma(D)$ and the fall speed $V_f(D)$ are known functions of diameter D, and the size distribution $N(D)$ is presumed unknown. The spectral functions are given by

$$S_{v1}(v)dv \propto \sigma(D)\nu_m^2(D)N(D)dD, \tag{26}$$

$$S_{v2}(v)dv \propto \sigma(D)N(D)dD, \tag{27}$$

$$S_{v12}(v)dv \propto \sigma(D)N(D)\rho_\alpha(D)\nu_m(D)\times\exp\{j[\delta(D)\pm 2\alpha(D)]\}dD. \tag{28}$$

The function ν^2 is related to drop size, elevation angle, and the fraction ρ_α of oriented scatterers and corresponds to the function H used by Warner and Rogers (1977),[1] which was based on calculations by McCormick and Hendry (1975), i.e.,

$$\nu^2(D,\rho_\alpha,\phi)=[\rho_\alpha\cos^4\phi+(8/15)(1-\rho_\alpha)]\times\exp(-10.26D^{-0.70}) \tag{29}$$

with D in millimeters. The subscript m in Eqs. (26) and (28) denotes values to be derived from the spectral functions. The propagation and range factor B_0 has been omitted, the cross-section function $\sigma(D)$ corresponds to the squared scattering amplitude $|S_{11}+S_{22}|^2$, and the quantity $N(D)dD$ is the number of drops of diameter D in the diameter increment dD, corresponding to the summation over all drops having the Doppler velocity v. Eq. (27) is the relation one would use in the interpretation of the Doppler spectrum from a single-channel (linearly polarized) coherent radar. It is the combination of $\sigma(D)$ and $N(D)$ in Eq. (27) together with the difficulty of separating air velocity from fallspeed that makes the single-channel methods of deducing drop size distribution uncertain.

The interpretation of the spectral functions is illustrated schematically in Fig. 1. Following the terminology of Bloomfield (1976) we define the coherency as

$$\mathrm{Coh}_v(v)=\frac{|S_{v12}(v)|}{[S_{v1}(v)S_{v2}(v)]^{\frac{1}{2}}}. \tag{30}$$

Based on Eqs. (26), (27), and (28), in the absence of propagation effects, the coherency equals the fraction $\rho_\alpha(v)$ of oriented scatterers as a function of measured Doppler velocity. The ratio of the spectral densities gives the power ratio as a function of Doppler velocity:

$$\frac{S_{v1}(v)}{S_{v2}(v)}=\nu_m^2(v). \tag{31}$$

The drop size as a function of measured Doppler velocity can then be determined as follows. At each spectral band, i.e., at each value of v, the value of $\rho_\alpha(v)$ and the elevation angle ϕ are used in Eq. (29) to obtain a function $\nu^2(D)$ for the particular value of v. This can then be inverted to the form $D(\nu^2)$ and the value of $\nu_m^2(v)$ from Eq. (31) used to obtain a diameter corresponding to the particular value of v. Since the fallspeed V_f as a function of drop size is known, the fallspeed can be determined as a function of Doppler velocity, and hence the Doppler component due to fallspeed V_{fd} as a function of Doppler velocity. In the ideal case of zero turbulence, the latter function can be extrapolated to zero fallspeed to obtain the Doppler component due to air velocity V_a. Practical approaches to the derivation of V_a are discussed in conjunction with the example presented below.

To this point no calibration has been required on the spectral functions. If the main channel spectrum is calibrated so that

$$\int_{-\infty}^{\infty} S_{v2}(v)dv=Z, \tag{32}$$

where Z is the reflectivity factor, then it can be used to obtain the drop size distribution. One method for achieving this result is illustrated in Fig. 1. The derived function $D(v)$ can be used to make the change of variables

$$S_{v2}(v)dv=S_{D2}(D)dD \tag{33}$$

and the known relation of backscatter cross section to diameter is used to obtain the drop size distribution $N(D)$. An alternate approach is to use the derived Doppler component due to air velocity V_a to shift the velocity scale of the power spectrum and then to use the relation of fallspeed to diameter to obtain the function $S_{D2}(D)$. The latter procedure is identical to that customarily used in the interpretation of power spectra from a single-channel coherent radar; in the present case, however, the air velocity V_a is derived directly from the radar measurements rather than from

[1] A numerical error in the original equation of Warner and Rogers was brought to our attention by G. C. McCormick.

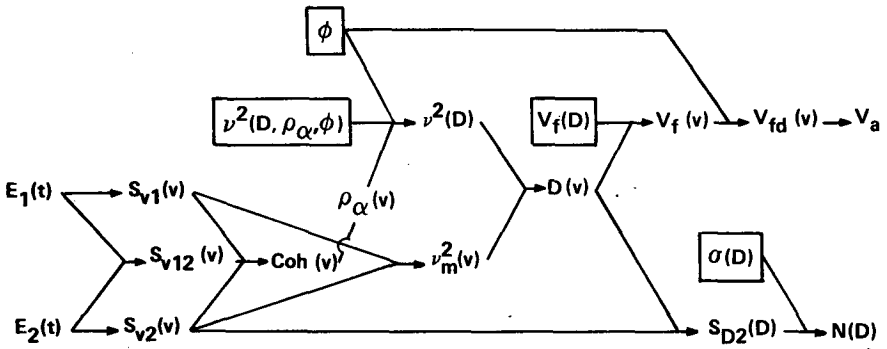

FIG. 1. Derivation of air velocity and drop size distribution from coherent polarization-diversity radar data. Measured signals are spectrum-analyzed and used to derive power ratio ν_m^2 and oriented fraction ρ_α as functions of Doppler velocity. With independently known functions and parameters (enclosed in rectangles), these yield the functional relationships and results shown. The propagation medium is assumed isotropic, so that differential propagation effects are omitted. See text for definitions of terms and full explanation of analytical procedure.

an independent statistical relationship. In practice, the function $D(v)$ is defined only over the velocity interval for which both power spectra were above the noise level, generally determined by the orthogonal channel spectrum S_1. Since the main channel spectrum may be expected to span a wider range of Doppler velocities than that of the orthogonal channel, the second method of deriving the drop size distribution is likely to be preferable to the method illustrated in Fig. 1. The change of variables shown in Eq. (33) requires that one can determine not only the value of D but also the derivative dv/dD at each value of v. This requirement imposes conditions on the continuity and smoothness of the spectral functions and the function $D(v)$ which need to be investigated.

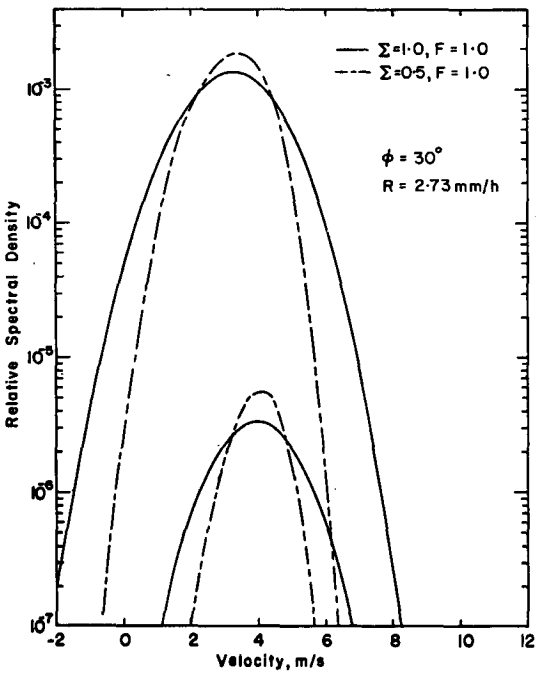

FIG. 2. Computed Doppler spectra for rainfall rate $R=2.73$ mm h^{-1} (reflectivity 30 dBz), elevation angle $\phi=30°$, and indicated values of turbulence parameter Σ and oriented fraction F, which corresponds to our ρ_α. The upper curves are for the main channel, and the lower ones are for the orthogonal channel (after Warner and Rogers, 1977).

Our formulation of the spectral functions implicitly assumes no velocity variance due to turbulence or wind shear. The effect of turbulence on the power spectra is illustrated by the computations of Warner and Rogers (1977). We used their spectra shown in Fig. 2 to derive the functions $\nu_m^2(v)$, $D(v)$, and ultimately the Doppler component due to fallspeed as a function of "measured" Doppler velocity. The results of our computations are shown in Table 1 and in Fig. 3. The turbulence parameter Σ represents the velocity standard deviation due to turbulence or wind shear. The effect of increasing turbulence is evident in that the empirically derived function $V_{fd}(v)$ approximates the theoretical relation more closely for $\Sigma=0.5$ than for $\Sigma=1.0$ at 30° elevation

TABLE 1. Parameters derived from computed Doppler spectra for given values of elevation angle ϕ and turbulence parameter Σ (fraction of oriented scatterers $\rho_\alpha=1$).

ϕ (deg)	Σ (m s^{-1})	v (m s^{-1})	10 log ν_m^2 (dB)	D (mm)	V_f (m s^{-1})	V_{fd} (m s^{-1})
30	1.0	1	−34.2	1.63	5.9	2.95
		2	−30.6	1.93	6.6	3.3
		3	−27.7	2.26	7.2	3.6
		4	−25.2	2.62	7.6	3.8
		5	−23.5	2.93	8.0	4.0
		6	−22.0	3.26	8.2	4.1
	0.5	2	−38.9	1.33	5.0	2.5
		3	−30.0	1.99	6.7	3.35
		4	−24.3	2.78	7.9	3.95
		5	−21.1	3.48	8.5	4.25
60	1.0	5	−39.5	2.00	6.7	5.8
		6	−36.4	2.37	7.3	6.3
		7	−33.7	2.80	7.8	6.8
		8	−31.7	3.22	8.2	7.1

angle. The results for $\Sigma=1.0$ are slightly better at 60° elevation than at 30° due to the larger spread of Doppler components due to fallspeed at the higher elevation angle.

The effects of turbulence on the computation of the Doppler component due to fallspeed can also be seen qualitatively in Fig. 2. Warner and Rogers (1977) pointed out that because the signal in the orthogonal channel is due to the larger, more aspherical, faster falling drops, the peak of its spectrum occurs at a higher Doppler velocity than that of the main channel spectrum. At Doppler velocities equal to or less than that of the peak of the main channel spectrum, the effect of increasing turbulence is to increase the magnitude of the orthogonal channel spectrum relative to the main channel spectrum. This leads to an overestimate of ν_m^2 and corresponding overestimates of the values of D, V_f and V_{fd}. At Doppler velocities equal to or greater than that of the peak of the orthogonal channel spectrum, the effect of increasing turbulence is to increase the magnitude of the main channel spectrum relative to the orthogonal channel spectrum. This leads to an underestimate of ν_m^2 and corresponding underestimates of the values of D, V_f and V_{fd}. At some value of Doppler velocity between those of the spectral peaks, the relative magnitudes of the spectra are such that the derived value of V_{fd} satisfies the theoretical relation $V_{fd}=v-V_a$. This intersection point, from which the air velocity can be derived by extrapolation of the theoretical relation to $V_{fd}=0$, could be determined approximately as the midpoint between the abscissae of the peaks of the two spectra. In practice, a statistical "best-fit" procedure between the derived relation and the theoretical relation may yield the best results.

At 31.3° elevation, i.e., where $\cos^4\phi=8/15$, the function ν^2 becomes independent of ρ_α. McCormick (private communication) has pointed out that the analysis we have described for observations in rain could be accomplished at this elevation angle without recourse to the cross spectrum, since the function $\rho_\alpha(v)$ is not required in Eq. (29). (At this elevation angle the cross spectrum continues to be essential for understanding hydrometeor microphysics, identifying the presence of ice-phase hydrometeors, and deriving propagation parameters.) At elevation angles less than 31.3° the effect of decreasing ρ_α is to decrease the signal power in the orthogonal channel. Above this elevation angle the signal power in the orthogonal channel increases with decreasing values of ρ_α. This is due to the fact that the vertically oriented raindrops yield the largest power in the orthogonal channel at 0° elevation and zero power in the orthogonal channel at 90° elevation, and that increasing randomness of orientation tends to make the power observed in the orthogonal channel at any elevation angle approach that which is observed at 31.3° elevation.

As a final illustration of the use of the spectral functions we have computed spectra and cross-spectrum for a mixture of rain and hail. Our model is defined as follows:

Rain:

$$N_R(D)=8\times10^6\exp(-2.53D), \quad R=10 \text{ mm h}^{-1}$$
(Marshall and Palmer, 1948)

$$\sigma_R(D)=(\pi^5/\lambda^4)|K|^2D^6, \quad |K|^2=0.97$$
$$V_{fR}(D)=9.43\{1-\exp[-(D/1.77)^{1.147}]\}$$
(Best, 1950)

$$\rho_{\alpha R}(D)=1$$
$$\nu_R^2(D,\rho_\alpha,\phi)=\cos^4\phi\exp(-10.26D^{-0.70})$$

Hail:

$$N_H(D)=3.1\times10^3\exp(-0.31D)$$ (Douglas, 1964)

$\sigma_H(D)$ after Herman and Battan (1961)

$$V_{fH}(D)=4.11D^{\frac{1}{2}}$$ (Martner and Battan, 1976)

$$\rho_{\alpha H}(D)=0$$
$$\nu_H^2(D,\rho_\alpha,\phi)=0.03$$
(corresponding to CDR = −15 dB).

Units are m^{-4}, m^2 and m s^{-1} but D is in millimeters in the equations for N, V_f and ν^2. The spectral functions are given by

$$S_{v1}(v)dv\propto\sigma_R(D)N_R(D)\nu_R^2(D)dD_R+\sigma_H(D)N_H(D)\nu_H^2(D)dD_h, \quad (34)$$

$$S_{v2}(v)dv\propto\sigma_R(D)N_R(D)dD_R+\sigma_H(D)N_H(D)dD_H, \quad (35)$$

$$S_{v12}(v)dv\propto\sigma_R(D)N_R(D)\rho_{\alpha R}(D)\nu_R(D)\times\exp[j(\delta\pm2\alpha)]dD_R+\sigma_H(D)N_H(D)\rho_{\alpha H}(D)\nu_H(D)\times\exp[j(\delta\pm2\alpha)]dD_H. \quad (36)$$

Using the model values for ρ_α we obtain the coherency

$$\text{Coh}_v(v)=\frac{\sigma_R(D)N_R(D)\nu_R(D)(dD_R/dv)}{\{[\sigma_RN_R\nu_R^2(dD_R/dv)+\sigma_HN_H\nu_H^2(dD_H/dv)]\times[\sigma_RN_R(dD_R/dv)+\sigma_HN_H(dD_H/dv)]\}^{\frac{1}{2}}}. \quad (37)$$

The total coherency is a power-weighted average of components due to rain having a coherency of unity and due to hail having a coherency of zero. The results of the calculations are shown in Fig. 4 for $\lambda=10$ cm and $\phi=30°$. The inflections in the spectra are due to the cutoff of the rain component at a Doppler velocity of 4.7 m s^{-1}, corresponding to a fallspeed of 9.4 m s^{-1}, and the fact that the scatter due to hail does not exceed the

scatter from rain at and below this velocity. With suitably chosen model distributions one could obtain spectra that did not have the inflection. The coherency illustrates the effect of the increasing fraction of hail with hydrometeor size and fallspeed. At low velocities the coherency is near unity, indicating that all the scatter in these bands is due to rain. Above about 2 m s^{-1} the scattering due to hail increases, and the coherency decreases to the point that the scattering is entirely due to hail, about 5 m s^{-1}.

If all the hail had fallspeeds less than 9.4 m s^{-1}, it could be distinguished from rain on the basis of the coherency. The coherency obtained from observations of rain would have a uniformly high value, whereas the presence of hail would result in a local decrease. Such a feature would provide not only an indicator of the presence of hail but also a measure of its size, according to its location on the velocity scale. The coherency would also provide an indicator of hail in observations at low elevation angles, where the Doppler component due to fallspeed is negligible.

5. Concluding remarks

We have described what appears to be a powerful technique for meteorological measurements. We have illustrated the use of this technique for deriving raindrop size distributions, separating Doppler components due to fallspeed and air velocity, and identifying the presence of hail.

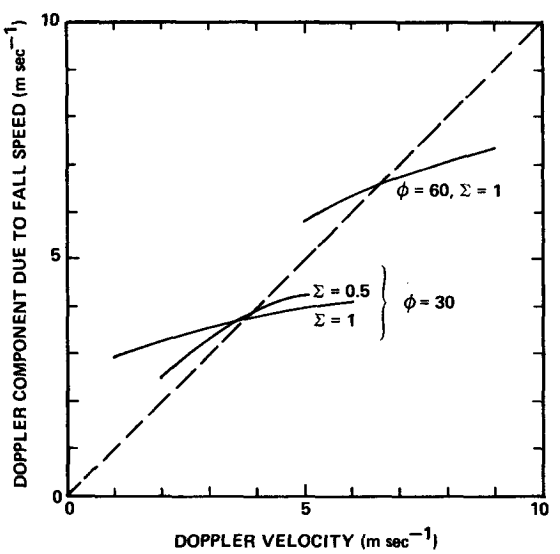

FIG. 3. Doppler components due to fallspeed derived from the computed spectra of Warner and Rogers (1977) and plotted against the Doppler velocity coordinate of the original spectra. Air velocity was assumed zero in the model, so that the total Doppler velocity is due to fallspeed and turbulence. The effect of the turbulence parameter Σ is evident at 30° elevation angle. Result at 60° elevation angle is better than at 30° because of the greater Doppler velocity spread due to fallspeeds. In the ideal case of zero turbulence, points would lie along the broken line.

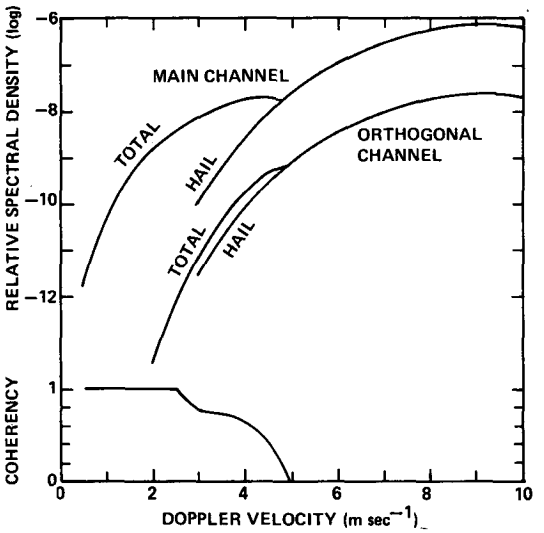

FIG. 4. Power spectra and coherency computed from rain and hail model described in the text. Signal in both channels below about 2 m s^{-1} is dominated by rain, as indicated both by the relative magnitudes of the spectra and by the coherency near unity. Above 2 m s^{-1} the signal component due to hail increases, with a resulting decrease in coherency to the point that the signals are due entirely to hail, above 5 m s^{-1}.

A coherent polarization-diversity radar could be of significant value in a wide variety of applications. It should be emphasized that the derivation of the Doppler component due to air velocity and the drop size distribution described in Section 3 applies to a single radar sampling volume. Thus, from a sequence of azimuth scans at constant elevation angles both horizontal and vertical variations in the drop size distribution can be documented, and the separation of Doppler components due to fallspeed and air velocity permits an unambiguous measure of the convergence as a function of altitude. A coherent polarization-diversity radar could also be used in conjunction with a single-channel coherent radar for improved velocity measurements in convective storms. In such an application, it would be preferable that all the radars have the polarization-diversity capability, as the relatively high elevation angles required for the analysis we have described restrict the effective surveillance range of a coherent polarization-diversity radar. Comparison of the polarization parameters derived from observations from different points would also be valuable for confirming suspected propagation effects. Research results in several closely related areas suggest the value of coherent polarization-diversity radar for observations of snow and ice crystals. Weiss and Hobbs (1975) related height variations of mean Doppler velocity to ice crystal habit by modeling the rates of change of particle size resulting from growth by vapor deposition and by riming. Sassen (1976) interpreted changes in depolarization ratios measured by lidar near the melting level in terms of the internal structure of the melting

hydrometeors and thus identified certain classes of ice-phase hydrometeors above the melting level. Hendry and McCormick (1976) discerned changes in orientation of ice crystals by thunderstorm electric fields from measurements with a 1.8 cm noncoherent polarization-diversity radar. These results also indicate that an empirical approach will be necessary for the application of coherent polarization-diversity radar to observations of snow and ice crystals.

We have not discussed the possible uses of the phase of the cross spectrum. This is defined by

$$\mathrm{Ph}(f)=\tan^{-1}\left[\frac{\mathrm{Im}[S_{12}(f)]}{\mathrm{Re}[S_{12}(f)]}\right] \tag{38}$$

and in the absence of propagation effects is given by $\delta(D)\pm 2\alpha(D)$, where the particular value of D is that corresponding to the scatterers which yield the Doppler shifted frequency f. In the absence of non-Rayleigh scattering ($\delta=0$), the spectral phase gives the orientation angle of the scattering medium as a function of Doppler velocity. Derivation of the spectral phase from measurements at alternating polarizations will provide the spectral distribution of δ, which may be useful for the identification of large hydrometeors.

For the sake of clarity in presenting these ideas, we have omitted the consideration of propagation effects. The limiting effects of differential propagation parameters are related to the rainfall rate in a complicated way, since the propagation parameter p appears as an additive term with the scattering amplitude ratio ν in the equations for the orthogonal channel spectrum S_1 and the cross spectrum S_{12}, and both increase with rainfall rate. The theoretical value of ν computed by Humphries (1974) for intense rain (reflectivity 55 dBZ) is about 0.18. Neglect of propagation effects would be justified for $p\lesssim 0.02$, which imposes an upper limit of path length through intense rain of about 0.75 km for observations at 10 cm (3 GHz) and even less for shorter wavelengths. For moderate rain (reflectivity 40 dBZ), Humphries obtained a value of $\nu=0.10$. A corresponding limit of p would be about 0.01, which limits the path length through moderate rain to about 2 km for wavelengths longer than about 5 cm (6 GHz) and about 1 km at 2 cm (15 GHz). These path limits are those for which propagation effects can be neglected; at somewhat greater distances valid information on the scattering medium may still be recoverable. An intriguing possibility for the investigation of propagation effects is the development of a spectral analog of the technique described by McCormick and Hendry (1975), by normalizing the cross spectrum by the main channel spectrum. The resulting function

$$\frac{S_{12}(f)}{S_2(f)}=\rho_\alpha(f)\nu(f)\exp\{j[\delta(f)\pm 2\alpha(f)]\}+2p\exp[j(\chi\pm 2\tau)] \tag{39}$$

includes a scattering term which is dependent on Doppler frequency and a propagation term which is not. Thus, the propagation term will dominate in some frequency bands but not in others, and it may be possible in some situations to compute the propagation term unambiguously.

We have developed expressions for the spectral functions based on deterministic functions of rain drop size. As was noted in Section 3, the range to the ith scatterer is the only random variable we have considered. In practice, the parameters v_i, ν_i and α_i will all be random variables because of turbulence, oscillation and tumbling, and hence the measured signals E_1 and E_2 and the spectral functions will all be random variables. The accuracy of the derived values of the power ratio $\nu_m^2(v)$ and the drop size $D(v)$ thus becomes dependent on the numerical procedures used in obtaining the spectral estimates. If spectral estimates with 95% confidence intervals of ± 2 dB are obtained, then the ratio ν_m^2 can be obtained with a 95% confidence interval smaller than ± 1 dB if the coherency is near unity. The drop sizes and fallspeeds can then be determined with confidence intervals of about 5 and 3%, respectively, for drops about 2 mm diameter, and about 11 and 1%, respectively, for drops about 6 mm diameter. Fig. 3 shows that in the presence of turbulence there will be a systematic deviation of the derived fallspeed from the theoretically expected values which can be greater than that due to statistical considerations. The full significance of the time-dependence of the parameters ν_i, δ_i and α_i, the interrelationships of confidence intervals and frequency resolution of the spectral functions, and the effects of numerical uncertainties on the derived physical quantities remain as major topics for further investigation. Ultimately, the practical limits due to radar design factors must also be determined.

Acknowledgments. We are grateful to R. R. Rogers of McGill University and C. Warner of the University of Virginia, whose referenced work provided the inspiration for this paper, and to K. M. Glover and M. J. Kraus of Air Force Geophysics Laboratory, who first questioned us concerning the information potential of a coherent polarization-diversity radar. Many improvements to the original manuscript were generated in discussions with D. Atlas of the National Aeronautics and Space Administration, R. E. Carbone of the National Center for Atmospheric Research, and R. R. Rogers. Support for this research was provided by AFGL under Contract F19628-77-C-0066.

REFERENCES

Anderson, R. S., 1975: Polarization measurements at 16.5 GHz in stratiform and convective precipitation. *Preprints 16th Radar Meteor. Conf.*, Houston, Amer. Meteor. Soc., 425–426.

Barge, B. L., 1972: Hail detection with a polarization diversity radar. Ph.D. dissertation and Sci. Rep. MW-71, Stormy Weather Group, McGill University, 80 pp.

Battan, L. J., 1977: Rain resulting from melting ice particles. *J. Appl. Meteor.*, **16**, 595–604.

——, and J. B. Theiss, 1972: Observed Doppler spectra of hail. *J. Appl. Meteor.*, **11**, 1001–1007.

——, and ——, 1975: Doppler spectra of rain in the cross-polarized plane. *Bull. Amer. Meteor. Soc.*, **56**, 1271–1272.

Best, A. C., 1950: Empirical formulae for the terminal velocity of water drops falling through the atmosphere. *Quart. J. Roy. Meteor. Soc.*, **76**, 302–311.

Bloomfield, P., 1976: *Fourier Analysis of Time Series: An Introduction.* Wiley, 258 pp.

Chernikov, A. A., V. A. Kapitanov and Yu. V. Mel'nichuk, 1973: A polarization dependence of Doppler spectra of precipitation radar returns. Abstract of paper presented at IUCRM Colloq., Nice, France.

Douglas, R. H., 1964: Hail size distribution. *Preprints 11th Conf. Radar Meteorology*, Boulder, Amer. Meteor. Soc., 146–149.

duToit, P. S., 1967: Doppler radar observations of drop sizes in continuous rain. *J. Appl. Meteor.*, **6**, 1082–1087.

Harris, F. I., 1977: The effects of evaporation at the base of ice precipitation layers: Theory and radar observations. *J. Atmos. Sci.*, **34**, 651–672.

Hendry, A., and G. C. McCormick, 1976: Radar observations of the alignment of precipitation particles by electrostatic fields in thunderstorms. *J. Geophys. Res.*, **81**, 5353–5357.

——, —— and B. L. Barge, 1976: The degree of common orientation of hydrometeors observed by polarization-diversity radars. *J. Appl. Meteor.*, **15**, 633–640.

Herman, B. M., and L. J. Battan, 1961: Calculations of Mie backscattering from melting ice spheres. *J. Meteor.*, **18**, 468–478.

Humphries, R. G., 1974: Depolarization effects at 3 GHz due to precipitation. Ph.D. dissertation and Sci. Rep. MW-82, Stormy Weather Group, McGill University, 81 pp.

Kropfli, R. A., and L. J. Miller, 1976: Kinematic structure and flux quantities in a convective storm from dual-Doppler radar observations. *J. Atmos. Sci.*, **33**, 520–529.

Marshall, J. S., and W. M. Palmer, 1948: The distribution of raindrops with size. *J. Meteor.*, **5**, 165–166.

Martner, B. E., and L. J. Battan, 1976: Calculations of Doppler radar velocity spectrum parameters for a mixture of rain and hail. *J. Appl. Meteor.*, **15**, 491–498.

McCormick, G. C., 1968: An antenna for obtaining polarization-related data with the Alberta Hail Radar. *Preprints 13th Radar Meteorology Conf.*, Montreal, Amer. Meteor. Soc., 340–347.

——, and A. Hendry, 1975: Principles for the radar determination of the polarization properties of precipitation. *Radio Sci.*, **10**, 421–434.

Musgrove, C., and M. Brook, 1975: Microwave echo fluctuations produced by vibrating water drops. *J. Atmos. Sci.*, **32**, 2001–2007.

Sassen, K., 1976: Polarization-diversity lidar returns from virga and precipitation. Anomalies and the bright band analogy. *J. Appl. Meteor.*, **15**, 292–300.

Sekhon, R. S., and R. C. Srivastava, 1971: Doppler radar observations of drop-size distributions in a thunderstorm. *J. Atmos. Sci.*, **28**, 983–994.

Warner, C., and R. R. Rogers, 1977: Polarization-diversity radar: Two theoretical studies. Sci. Rep. MW-90, Stormy Weather Group, McGill University, 47 pp.

Weiss, R. R., and P. V. Hobbs, 1975: The use of a vertically pointing pulsed Doppler radar in cloud physics and weather modification studies. *J. Appl. Meteor.*, **14**, 222–231.